

# On Domain-Specific Post-Training for Multimodal Large Language Models

Daixuan Cheng<sup>1</sup> Shaohan Huang<sup>2</sup> Ziyu Zhu<sup>1,3</sup> Xintong Zhang<sup>1,4</sup> Wayne Xin Zhao<sup>5</sup>  
 Zhongzhi Luan<sup>2</sup> Bo Dai<sup>1✉</sup> Zhenliang Zhang<sup>1✉</sup>

<sup>1</sup>State Key Laboratory of General Artificial Intelligence, BIGAI <sup>2</sup>Beihang University

<sup>3</sup>Tsinghua University <sup>4</sup>Beijing Institute of Technology <sup>5</sup>Renmin University of China

<https://huggingface.co/AdaptLLM>

## Abstract

Recent years have witnessed the rapid development of general multimodal large language models (MLLMs). However, adapting general MLLMs to specific domains, such as scientific fields and industrial applications, remains less explored. This paper systematically investigates domain adaptation of MLLMs through post-training, focusing on data synthesis, training pipelines, and task evaluation. (1) **Data Synthesis:** Using open-source models, we develop a visual instruction synthesizer that effectively generates diverse visual instruction tasks from domain-specific image-caption pairs. Our synthetic tasks surpass those generated by manual rules, GPT-4, and GPT-4V in enhancing the domain-specific performance of MLLMs. (2) **Training Pipeline:** While the two-stage training—initially on image-caption pairs followed by visual instruction tasks—is commonly adopted for developing general MLLMs, we apply a single-stage training pipeline to enhance task diversity for domain-specific post-training. (3) **Task Evaluation:** We conduct experiments in two domains, biomedicine and food, by post-training MLLMs of different sources and scales (e.g., Qwen2-VL-2B, LLaVA-v1.6-8B, Llama-3.2-11B), and then evaluating MLLM performance on various domain-specific tasks. To support further research in MLLM domain adaptation, we will open-source our implementations.

## 1. Introduction

Progress toward building general-purpose agents [20, 58] relies critically on the ability to handle multimodal tasks. The recent success of large language models (LLMs) [5, 12, 44] has accelerated the development of multimodal large language models (MLLMs) [2, 16, 23, 24, 28, 35, 43, 52, 54]. By aligning visual encoders [37] with LLMs, MLLMs have shown impressive capabilities in addressing vision-language tasks in general scenarios. However, their ex-

✉ Corresponding Author.

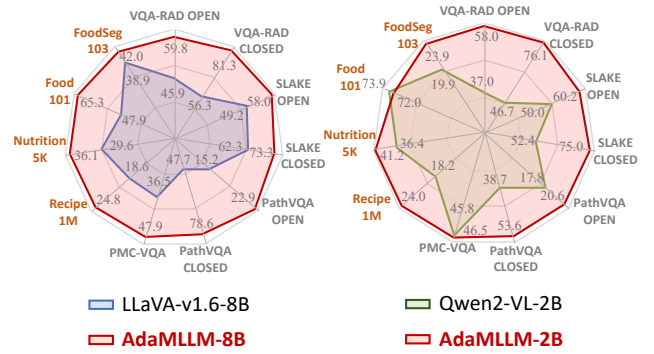


Figure 1. **Domain-Specific Performance of AdaMLLM and General MLLM.** For each of the two domains—biomedicine and food—we conduct post-training to adapt the general MLLM to the target domain and evaluate model performance on various domain-specific tasks. Biomedicine and food tasks are colored gray and orange, respectively.

pertise plummets in specialized domains due to insufficient domain-specific training [11]. For instance, scientific fields require learning from specialized images and terminology not commonly found in general scenarios [31, 39, 40, 56]; and industrial applications face privacy constraints that limit data access for training general MLLMs [3, 50].

Domain-specific training for MLLMs requires diverse visual instruction tasks infused with domain knowledge [21]. Recent efforts in this area [7, 22, 32] typically follow the data synthesis and training pipeline used for general training. For data synthesis, manual rules or strong models are employed to generate domain-specific tasks. However, rule-based methods can limit task diversity [10], closed-source models [1, 34] may pose privacy concerns, and open-source models can be constrained by insufficient domain expertise. For training, many works use a two-stage pipeline—first training on image-caption pairs, then on visual instruction tasks [28]. However, tasks in specialized domains are often limited, and splitting them into two stages can further reduce task diversity within each stage.

In this paper, we systematically investigate domain-

specific data synthesis and training pipeline for MLLM post-training. While domain-specific image-caption pairs are relatively accessible, domain-specific visual instruction tasks are much harder to obtain [22]. To bridge this gap, we develop a visual instruction synthesizer to extract tasks from image-caption pairs. Fine-tuned on a seed data collection encompassing various domains and tasks, our synthesizer can effectively leverage domain knowledge in the image-caption source to generate diverse instruction-response pairs<sup>1</sup>. To check the accuracy of synthetic responses, rather than directly verifying each response against the instruction—which requires extensive expertise—we propose selecting tasks with inherently consistent responses. This improves accuracy while reducing the need for expert annotation. Although generated from open-source models, our synthetic tasks improve model performance more effectively than those generated by manual rules [32], GPT-4 [22], or GPT-4V [7]. Using our synthetic data, we propose a single-stage training pipeline that combines the synthetic task with the image-caption pair in each training example, avoiding the limitations from two-stage training. This simple approach enriches task diversity during training and leads to better performance in most experiments.

We conduct experiments in two domains: biomedicine and food, on general MLLMs of different sources and scales, such as Qwen2-VL-2B [45], LLaVA-v1.6-8B [27], and Llama-3.2-VL-11B [14]. As shown in Figure 1, our resulting model, AdaMLLM (for **Adapted Multimodal Large Language Model**), consistently outperforms the general MLLMs in various domain-specific tasks.

In summary, our contributions include:

- We investigate domain-specific post-training for MLLMs and open-source our implementations.
- We develop a visual instruction synthesis approach based on open-source models, capable of generating diverse tasks from domain-specific image-caption pairs while reducing the need for domain expertise.
- We propose a single-stage post-training method to enhance task diversity during the training phase.
- Our experiments demonstrate the effectiveness of our method in improving MLLM performance across various tasks in two domains: biomedicine and food.

## 2. Related Work

We discuss related work on data collection and training pipelines for developing domain-specific MLLMs.

**Domain-Specific Data** Initially, Med-Flamingo [33] utilizes multimodal paired and interleaved data. With the rise of visual instruction tuning for general MLLMs [28],

research has shifted to synthesizing domain-specific visual instruction data, following approaches for general MLLMs [21, 59]. These approaches fall into two categories: (1) transforming existing datasets into visual instruction formats: LLaVA-Chef [32] and FoodLMM [53] convert domain-specific datasets [38] using manual rules or GPT-4; (2) prompting closed-source models to generate visual instruction tasks from images/annotations: Med-VInT [57], LLaVA-Med [22] and PubMedVision [7] employ GPT-3.5, GPT-4, and GPT-4V, respectively. Our work aligns with the second category in synthesizing data based on image-caption pairs, but we utilize open-source models and effectively synthesize tasks of greater diversity.

**Domain-Specific Training** One type of domain-specific training begins with an unaligned LLM and visual encoder. Similar to the development of general MLLMs, this method uses domain-specific datasets, possibly mixed with general datasets, to align the LLM with the encoder [7, 57]. Another type is post-training, which starts with a well-aligned general MLLM [7, 22, 32]. Compared to training from an unaligned LLM and vision encoder, post-training is more efficient in terms of data and computation, making it our preferred method. In domain-specific post-training, many previous works [7, 22, 32] adopt the two-stage training pipeline originally proposed for general MLLMs: first on image-caption pairs, then on visual instruction tasks. We simplify this into a single-stage training pipeline to enhance task diversity within the training phase.

## 3. Method

We adapt MLLMs to domains via post-training on domain-specific datasets. As shown in Figure 2, we begin by synthesizing domain-specific tasks using a unified visual instruction synthesizer, followed by a consistency-based data filter. These synthetic tasks are then combined with image-captioning tasks into a single stage for post-training.

### 3.1. Domain-Specific Visual Instruction Synthesis

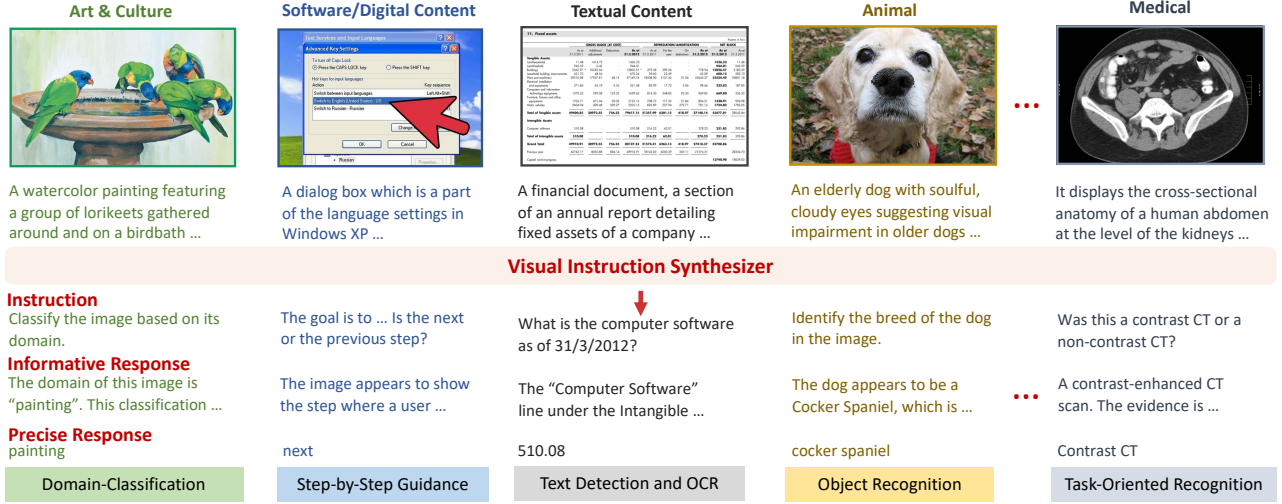
The effectiveness of visual instruction tasks depends on diversity and accuracy, with domain knowledge being essential for domain adaptation [21]. To meet these requirements, we propose a data synthesis approach comprising two main components: a visual instruction synthesizer that generates diverse tasks infused with domain-specific knowledge, and a consistency-based filter to enhance accuracy.

#### 3.1.1. Visual Instruction Synthesizer

While domain-specific image-caption pairs are widely accessible, domain-specific visual instruction tasks are much harder to obtain [22]. Inspired by *Instruction Pre-Training* [10] which develops a model to extract tasks from texts, we fine-tune an MLLM to generate diverse tasks

<sup>1</sup>We use “task” and “instruction-response pairs” interchangeably, with “instruction” as task input and “response” as task output.

## (A) Fine-Tune a Visual Instruction Synthesizer across Domains and Tasks



## (B) Synthesize Domain-Specific Tasks to Post-Train General MLLMs

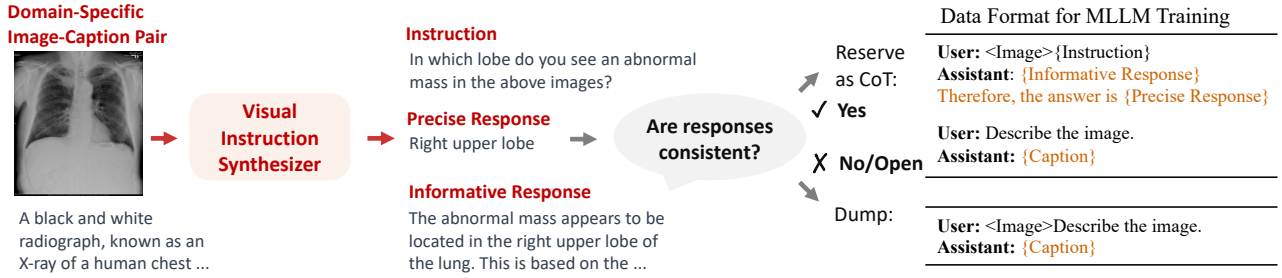


Figure 2. **Method Overview.** (A) We fine-tune a unified visual instruction synthesizer that generates diverse tasks based on image-caption pairs across various domains. (B) Using this synthesizer, we synthesize tasks based on domain-specific image-caption pairs and then apply a consistency-based data filter. The filtered synthetic tasks, combined with the original image captioning tasks, are employed to train general MLLMs through a single-stage post-training process, MLLM training loss is computed only on the part colored in orange.

based on image-caption pairs across various domains, developing a *visual instruction synthesizer*. Instead of generating domain-specific tasks from scratch, which requires significant expertise, our synthesizer extracts tasks from existing data, thus reducing the reliance on domain expertise from human experts or strong models [1, 34, 41]. Furthermore, we incorporate specific designs to handle situations where the synthesizer struggles to comprehend the image.

**Seed Data across Domains and Tasks** We convert a combination of VisionFLAN [51] and ALLaVA [6] into the seed data for fine-tuning our visual instruction synthesizer. As shown in part (A) of Figure 2, each seed data example includes an image-caption pair as input and a related task triplet—comprising an instruction, an informative response, and a precise response—as output. Specifically, for each image, both the instruction and precise response are annotated by human experts, while the caption and informative response are generated by GPT-4V. Compared to the precise response which is often a single phrase, the infor-

<b>User:</b> <Image>Describe the image.
<b>Assistant:</b> {Caption}
<b>User:</b> Answer with a precise response. {Instruction}
<b>Assistant:</b> {Precise Response}
<b>User:</b> Answer with an informative response. {Instruction}
<b>Assistant:</b> {Informative Response}

Table 1. **Data Format for Synthesizer Tuning.** The prefixes “User” and “Assistant” are determined by synthesizer’s chat template. **Tuning loss** is computed only on the part colored in orange.

mative response contains many more details, such as chain-of-thought reasoning [48]. The seed data encompass a wide range of image domains (e.g., art, software) and task types (e.g., object recognition, domain classification). Details on data construction and distribution are in Appendix A.

**Generalization-Enhanced Multitask Tuning** Using the seed data, we conduct multitask fine-tuning on an open-source MLLM to generate task triplets based on the corresponding image-caption pairs. As shown in Table 1, each

seed data example is converted into a multi-turn conversation to fit the MLLM’s conversational format. The first turn presents the image-caption pair. Then the task triplet is divided into two conversational turns. Each turn starts with a prompt requesting either a precise response or an informative response, followed by the instruction. The order of the precise and informative response turns is shuffled randomly. We calculate the tuning loss only on the turns related to the task triplet, ensuring the synthesizer focuses on them.

Furthermore, since generalizing to unseen image types is substantially more challenging than to unseen text types, we replace 10% of the images with a blank image during tuning. This simulates cases where the synthesizer struggles to interpret the image, encouraging it to rely more on the caption when facing difficulties in image comprehension.

**Task Synthesis for Target Domain** After tuning, we use the synthesizer to generate task triplets from image-pairs in the target domain. For each image-caption pair, we input it into the synthesizer using the conversational format in Table 1 and extract the task triplet from the output accordingly.

### 3.1.2. Consistency-Based Filter

Developed from an open-source model without sufficient domain expertise, our synthesizer inevitably produces some inaccurate responses, necessitating data filtering. To reduce reliance on experts for validation, we propose filtering tasks based on inherent consistency. This is inspired by ensemble methods [13] and self-consistency decoding [46], enhancing accuracy while reducing the need for expert annotation.

As shown in part (B) in Table 2, we prompt an open-source language model to classify each “instruction-precise response-informative response” triplet into one of three categories: consistent, inconsistent, or open. The consistent and inconsistent categories indicate whether the precise and informative responses align, while the open category indicates tasks that request open-ended responses (e.g., image captions or background information). The prompt template is in Figure 6 in Appendix. We discard triplets classified as inconsistent, as they show low synthesizer confidence, and those classified as open due to their ambiguity.

For consistent triplets, we combine the informative and precise responses into a chain-of-thought (CoT) format using diverse templates from [29]. The informative response serves as the reasoning process, and the precise response serves as the final conclusion. This ensures both informativeness and accuracy, balancing the concise responses typical of academic datasets with the more detailed responses preferred by humans [26, 51].

## 3.2. Domain-Specific Single-Stage Post-Training

General MLLM training typically contains multiple stages: first on image-caption pairs, then on visual instruction

tasks [28]. This pipeline has also been applied in domain-specific post-training [7, 22, 32]. However, task diversity in domain-specific training is often more limited than in general training, and splitting the training into two stages may further reduce diversity within each stage, negatively impacting the task generalization of the trained models [47]. Moreover, we empirically find that two-stage training can lead the model to catastrophically forget the knowledge/task learned from the first stage when transitioning to the second stage, resulting in worse final performance [30]. To mitigate this, we propose combining the training data into a single stage. As shown in part (B) of Figure 2, each training example can include two tasks:

- *Image Captioning Task*: The image-caption pair is converted into an image captioning task [28]. A question prompting the MLLM to describe the image is randomly chosen from a pool in [6] as the task instruction, with the original caption as the ground-truth response.
- *Synthetic Visual Instruction Task*: For each image-caption pair with a synthetic task after filtering, we combine it with the image captioning task in a multi-turn format, with the task order randomized. If no synthetic task remains, only the image captioning task is used.

Following [28], we train on the data using the next-token prediction objective [36], computing loss only on the response part of each instruction-response pair.

## 4. Experiment Settings

Given current data availability, we conduct experiments in two domains: biomedicine and food. For each domain, we perform post-training to adapt general MLLMs and evaluate model performance on various domain-specific tasks.

**Image-Caption Data Source** For biomedicine, we use two sources from PubMed Central<sup>2</sup>: (1) PMC<sup>Raw</sup> [55] from LLaVaMed [22], comprising 470K available images with human-annotated captions, and (2) PMC<sup>Refined</sup> from PubMedVision [7], featuring 510K image-caption pairs where the captions have been refined by GPT-4V. For food domain, we convert Recipe1M [38] dataset into image-caption pairs. Each recipe is matched with one image and converted to a caption using templates from [32]. Recipes without images are removed, resulting in 130K image-caption pairs.

**Visual Instruction Synthesis** Our vision instruction synthesizer is fine-tuned from the open-source version [8] of LLaVA-v1.6-Llama3-8B [27]. For the consistency-based filter, we prompt Llama-3-8B [14] to evaluate the consistency of each synthesized task triplet. On average, about 30% of the task triplets are reserved after filtering. Details on implementations and synthetic data are in Appendix B.

<sup>2</sup><https://www.ncbi.nlm.nih.gov/pmc/>



Biomedicine	SLAKE		PathVQA		VQA-RAD		PMC-VQA
	OPEN	CLOSED	OPEN	CLOSED	OPEN	CLOSED	
GPT-4o	59.1	71.6	24.1	76.0	51.6	64.0	56.7
<b>LLaVA-v1.6-8B</b>	49.2	62.3	15.2	47.7	45.9	56.3	36.5
LLaVA-Med-8B	43.4	50.2	10.1	59.2	35.0	62.5	37.1
PubMedVision-8B	50.0	68.3	17.0	67.5	43.3	67.3	40.4
AdaMLLM-8B from PMC <sup>Raw</sup>	<u>56.8</u>	<b>76.4</b>	<u>19.7</u>	<b>79.3</b>	<u>51.0</u>	<u>80.5</u>	<u>44.3</u>
AdaMLLM-8B from PMC <sup>Refined</sup>	<b>58.0</b>	<u>73.3</u>	<b>22.9</b>	<u>78.6</u>	<b>59.8</b>	<b>81.3</b>	<b>47.9</b>
<b>Qwen2-VL-2B</b>	50.0	52.4	17.8	38.7	37.0	46.7	<u>45.8</u>
LLaVA-Med-2B	43.4	55.5	11.8	60.1	37.1	58.8	41.2
PubMedVision-2B	45.2	63.2	18.2	<b>64.7</b>	41.3	67.3	43.2
AdaMLLM-2B from PMC <sup>Raw</sup>	<u>53.2</u>	<b>75.2</b>	<u>20.1</u>	<u>63.8</u>	<u>49.8</u>	<u>74.6</u>	43.5
AdaMLLM-2B from PMC <sup>Refined</sup>	<b>60.2</b>	<u>75.0</u>	<b>20.6</b>	<u>53.6</u>	<b>58.0</b>	<b>76.1</b>	<b>46.5</b>
<b>Llama-3.2-11B</b>	56.2	63.9	<u>22.7</u>	72.1	46.9	63.6	<b>51.9</b>
LLaVA-Med-11B	47.6	58.7	14.6	69.5	38.0	69.1	47.5
PubMedVision-11B	49.1	74.3	19.3	70.9	46.2	73.9	47.1
AdaMLLM-11B from PMC <sup>Raw</sup>	<u>56.7</u>	<b>77.6</b>	22.2	<b>87.3</b>	<u>55.0</u>	<u>76.1</u>	<u>49.9</u>
AdaMLLM-11B from PMC <sup>Refined</sup>	<b>59.5</b>	<u>76.4</u>	<b>24.3</b>	<u>84.9</u>	<b>57.4</b>	<b>79.8</b>	<b>51.9</b>

Table 2. **Biomedicine Task Performance** of general MLLMs and MLLMs after domain-adaptive training. We mark the best performance **bold** and the second-best underlined. The image-caption sources for AdaMLLM from PMC<sup>Raw</sup> and AdaMLLM from PMC<sup>Refined</sup> are PMC<sup>Raw</sup> and PMC<sup>Refined</sup>, respectively.

**Post-Training** Using synthetic data from the LLaVA-v1.6-Llama3-8B-based synthesizer, we conduct domain-specific post-training on LLaVA-v1.6-Llama3-8B itself. Besides, we use the same synthetic data to post-train Qwen2-VL-2B-Instruct [45] and Llama-3.2-11B-Vision-Instruct [14] to assess effectiveness across different models and scales. For simplicity, we refer to these models as LLaVA-v1.6-8B, Qwen2-VL-2B, and Llama-3.2-11B, respectively. Training details are in Appendix C.

**Task Evaluation** We evaluate MLLMs on domain-specific tasks without further fine-tuning. For biomedicine, we evaluate on SLAKE [25], PathVQA [15], VQA-RAD [19], and PMC-VQA [57]. For food domain, we evaluate on Recipe1M [38], FoodSeg103 [49], Food101 [4], and Nutrition5k [42]. Details are in Appendix E.

**Baseline** For biomedicine domain, we compare with two baselines: (1) LLaVA-Med [22] which uses text-only GPT-4 to synthesize tasks from PMC<sup>Raw</sup>, and (2) PubMedVision [7] which uses GPT-4V to synthesize tasks from PMC<sup>Refined</sup>. For food domain, we compare with LLaVA-Chef [32] which uses manual rules to transform image-recipe pairs from Recipe1M into multiple tasks. All baseline methods employ two-stage post-training.

## 5. Main Results

**Overall Performance** Tables 2 and 3 compare our models (AdaMLLM) with others in the biomedicine and food

Food	Recipe	Nutrition	Food101	FoodSeg
GPT-4o	26.1	46.6	89.4	61.9
<b>LLaVA-v1.6-8B</b>	18.6	<u>29.6</u>	<u>47.9</u>	<u>38.9</u>
LLaVA-Chef-8B	<u>23.1</u>	29.1	46.8	14.5
AdaMLLM-8B	<b>24.8</b>	<b>36.1</b>	<b>65.3</b>	<b>42.0</b>
<b>Qwen2-VL-2B</b>	18.2	<u>36.4</u>	<b>73.9</b>	<u>19.9</u>
LLaVA-Chef-2B	<b>24.1</b>	24.5	68.8	7.7
AdaMLLM-2B	<u>24.0</u>	<b>41.2</b>	<u>72.0</u>	<b>23.9</b>
<b>Llama-3.2-11B</b>	23.7	<u>40.0</u>	80.8	<b>47.6</b>
LLaVA-Chef-11B	<u>25.7</u>	26.2	<u>82.1</u>	16.7
AdaMLLM-11B	<b>26.1</b>	<b>41.0</b>	<b>82.2</b>	<u>42.0</u>

Table 3. **Food Task Performance** of general MLLMs and MLLMs after domain-adaptive training. We mark the best performance **bold** and the second-best underlined.

domains, using GPT-4o [17] as a reference. Our method consistently enhances MLLM performance, outperforming baseline models across various domain-specific tasks. Although our synthesizer is based on LLaVA-v1.6-8B, we observe consistent improvements on Qwen2-VL-2B and Llama-3.2-11B, demonstrating its effectiveness across different models and scales. Among the evaluated tasks, VQA-RAD and Recipe1M can be regarded as partially seen tasks, with VQA-RAD included in our seed data for fine-tuning the synthesizer and Recipe1M included in the image-caption source<sup>3</sup>. Nevertheless, AdaMLLM shows consistent gains on other unseen tasks, demonstrating its task generalization capabilities in the target domain.

<sup>3</sup>Test/validation sets of VQA-RAD and Recipe1M are not included.

Image-Caption	Recipe1M				PMC <sup>Raw</sup>				PMC <sup>Refined</sup>			
	Two-stage		Single-stage		Two-stage		Single-stage		Two-stage		Single-stage	
	Rule	Ours	Rule	Ours	GPT-4	Ours	GPT-4	Ours	GPT-4V	Ours	GPT-4V	Ours
LLaVA-v1.6-8B	28.4	<b>29.0</b>	34.1	<b>42.0</b> ↑	42.5	<b>55.6</b>	46.1	<b>58.3</b> ↑	50.5	<b>58.6</b>	55.5	<b>60.3</b> ↑
Qwen2-VL-2B	31.3	<b>38.2</b>	31.9	<b>40.3</b> ↑	44.0	<b>55.5</b>	41.3	<b>54.3</b> ↓	49.0	<b>59.5</b>	51.6	<b>55.7</b> ↓
Llama-3.2-11B	37.7	<b>40.9</b>	36.6	<b>47.8</b> ↑	49.3	<b>59.2</b>	48.8	<b>60.7</b> ↑	54.4	<b>60.3</b>	53.7	<b>62.0</b> ↑

Table 4. **Domain-Specific Task Performance of MLLMs after Post-Training** with different synthetic data and training pipelines. We report the average performance in each domain, with detailed results in Table 14 in Appendix. When the image-caption source and training pipeline are fixed, synthetic data of better performance are marked in **bold**. When the image-caption source is fixed and our synthetic data are used, numbers marked with ↑ indicate that single-stage training outperforms two-stage training, while ↓ indicates the opposite.

	Ours	w/o Blank Image	w/o Consistency Filter		w/o Synthetic Task	w/o Image Caption	General Task	General Task + Domain Caption
			Precise	Informative				
BioMed.	<b>58.3</b>	55.8	31.2	44.4	26.7	54.2	49.8	55.3
Food	<b>42.0</b>	35.9	37.9	37.6	25.6	36.8	36.0	38.6

Table 5. **Ablation Results.** “w/o Blank Image” fine-tunes the synthesizer without replacing 10% of images with blank ones. “w/o Consistency Filter” removes the consistency-based filter and trains with either precise or informative responses. “w/o Synthetic Task” removes synthetic task, and “w/o Image Caption” removes image captioning task. “General Task” trains on seed data processed into our task format, “General Task + Domain Caption” mixes the processed seed data with domain-specific image-caption pairs.

### Comparison of Synthetic Task and Training Pipeline

In addition to the overall comparison, we assess the effectiveness of our synthetic visual instruction tasks and single-stage training separately by varying one factor at a time. As shown in Table 4, we conduct both two-stage and single-stage post-training with synthetic tasks generated by different methods: manual rules in LLaVA-Chef, GPT-4 in LLaVA-Med, and GPT-4V in PubMedVision. Our synthetic tasks consistently outperform others across both training pipelines. Furthermore, with our synthetic tasks, single-stage training surpasses two-stage training in most of the experiments. We discuss in Table 14 in Appendix, inferring that two-stage training leads the model to forget the knowledge/task learned in the first stage when transitioning to the second stage, resulting in worse performance across tasks.

## 6. Ablations

To evaluate the effectiveness of each component in our method, we conduct ablations to post-train LLaVA-v1.6-8B with different settings. We report the average task performance within each domain for the trained models in Table 5. The image-caption sources for the biomedicine and food domains are PMC<sup>Raw</sup> and Recipe1M, respectively.

**Visual Instruction Synthesis** To simulate scenarios where the model struggles to interpret the image, we replace 10% of the images with blank images during the fine-tuning of visual instruction synthesizer. The impact of this strategy is demonstrated in Table 5, where removing this design results in a decline in model performance.

To improve response accuracy, we design a consistency-based filter to select tasks with inherent consistency and combine the informative and precise responses into a CoT format. As shown in Table 5, removing this filter results in decreased model performance, regardless of whether the response contains only precise or informative content.

**Single-Stage Post-Training** Our motivation for combining the synthetic task with the image captioning task into a single stage is to enhance training task diversity. This efficacy is evident in the ablation results in Table 5, where removing either the synthetic task or the image captioning task from the training data harms the model performance.

**Domain Knowledge** Our domain-specific visual instruction tasks incorporate both domain knowledge and visual instruction task format. To evaluate the contributions of domain knowledge, we conduct a comparison with general visual instruction tasks. Our seed data for fine-tuning the synthesizer, which contains diverse tasks across various domains, serves as the source for general tasks. To ensure alignment in visual instruction task format, we apply our consistency-based filter to process and reformat the seed data into our format. As shown in Table 5, our method outperforms both settings that utilize general tasks, underscoring the effectiveness of incorporating domain knowledge.

## 7. Analysis

We conduct a detailed analysis of our approach for domain-specific visual instruction synthesis and the synthesized

Finetune Input	-	Image	Caption	Image + Caption	
<i>Blank Image</i>	-	-	-	✗	✓
Diversity	52.5	68.0	75.2	81.0	<b>85.5</b>
Knowledge	72.5	95.0	93.8	97.5	<b>98.1</b>
Complexity	43.8	77.9	75.3	80.0	<b>83.2</b>
Accuracy	63.8	60.0	65.6	66.3	<b>71.3</b>

Table 6. **Quality of Synthetic Tasks by Different Visual Instruction Synthesizers**, assessed in terms of task diversity, domain knowledge utilization, task complexity, and response accuracy. Column 1 presents results from the MLLM without fine-tuning. Columns 2-5 show results after fine-tuning the MLLM using our seed data to synthesize tasks based on different inputs. Besides, Column 5 replaces 10% of the images with blank images.

	w/o Filter			w/ Filter	
	Consist.	Precise Acc	Info. Acc	Consist.	Acc
BioMed.	30.3	64.3	61.0	92.2	75.1
Food	35.7	77.2	75.5	97.1	84.3

Table 7. **Quality of Responses with/without Using Consistency-Based Filter**, assessed in terms of consistency between precise and informative responses (Consist.), accuracy of precise responses (Precise Acc), accuracy of informative responses (Info. Acc), and accuracy of combined responses (Acc).

data to understand their impact on model performance.

## 7.1. Domain-Specific Visual Instruction Synthesis

**Visual Instruction Synthesizer** We fine-tune an MLLM to synthesize tasks from image-caption pairs and incorporate a design where 10% of the images are replaced with blank images. To evaluate the effectiveness, we compare tasks generated by synthesizers with different designs using a validation set from our seed data. Specifically, we conduct human evaluation of data quality in the following aspects (detailed scoring criteria are provided in Appendix D):

- *Task Diversity*: Classifies each instruction-response pair as one of the common visual instruction task types and reports the number of distinct types normalized by the total number of common task types.
- *Domain Knowledge Utilization*: Measures the extent to which domain-specific knowledge from the image is utilized to complete the task.
- *Task Complexity*: Assesses task complexity, with higher scores for tasks requiring reasoning and instruction-following abilities.
- *Response Accuracy*: Evaluates how accurately the response addresses the instruction.

The results in Table 6 indicate that fine-tuning for task synthesis using either image [59] or caption [10] inputs yields improvements in most aspects. Our design, which employs both image and caption inputs, leads to even higher performance. Besides, replacing 10% of the images with

Image-Caption	Recipe1M		PMC <sup>Raw</sup>		PMC <sup>Refined</sup>	
	Rule	Ours	GPT-4	Ours	GPT-4V	Ours
Diversity	23.5	<b>52.9</b>	47.1	<b>58.8</b>	64.7	<b>76.5</b>
Knowledge	20.9	<b>21.9</b>	44.9	<b>58.9</b>	<b>67.7</b>	63.2
Complexity	38.4	<b>69.9</b>	41.7	<b>83.2</b>	49.6	<b>80.5</b>
Accuracy	<b>98.7</b>	84.3	<b>84.4</b>	75.1	<b>87.5</b>	79.6

Table 8. **Quality of Synthetic Tasks** by our method, manual rules, GPT-4, and GPT-4V, assessed in terms of task diversity, domain knowledge utilization, task complexity, and response accuracy.

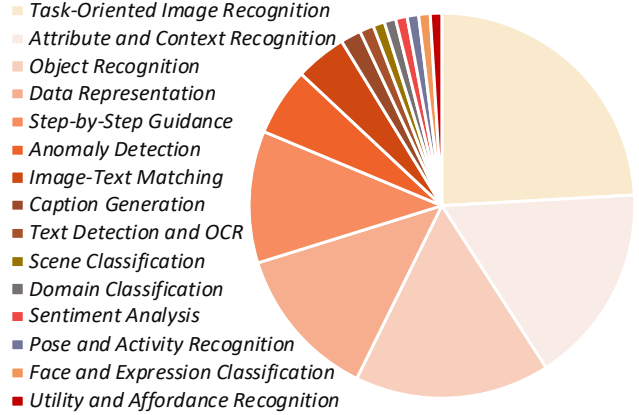


Figure 3. **Task Type Distribution** of all our synthetic tasks based on three image-caption sources.

blank ones achieves the highest quality across all metrics.

**Consistency-Based Filter** Our consistency-based filter is designed to select tasks with inherent consistency, thereby increasing data accuracy. As shown in Table 7, using the filter significantly increases the consistency between precise and informative responses, making the combination of them in the chain-of-thought format reasonable. As a result, the filter successfully increase response accuracy of the selected data by about 10% in both domains.

## 7.2. Domain-Specific Synthetic Data

**Quantitative Analysis** Table 8 presents the data quality scores for synthetic tasks generated by different methods. Our tasks are diverse and complex, demonstrating a high utilization of domain knowledge. The distribution of task types for all our instruction-response pairs is displayed in Figure 3. This explains the effectiveness of our method in enhancing MLLM performance across domain-specific tasks. However, our method underperforms the baselines in terms of response accuracy, with manual rules achieving nearly 100% accuracy and GPT-4 and GPT-4V reaching around 85%. This may because of the increased complexity of our synthesized tasks, which make generating accurate responses more challenging. These results indicate the

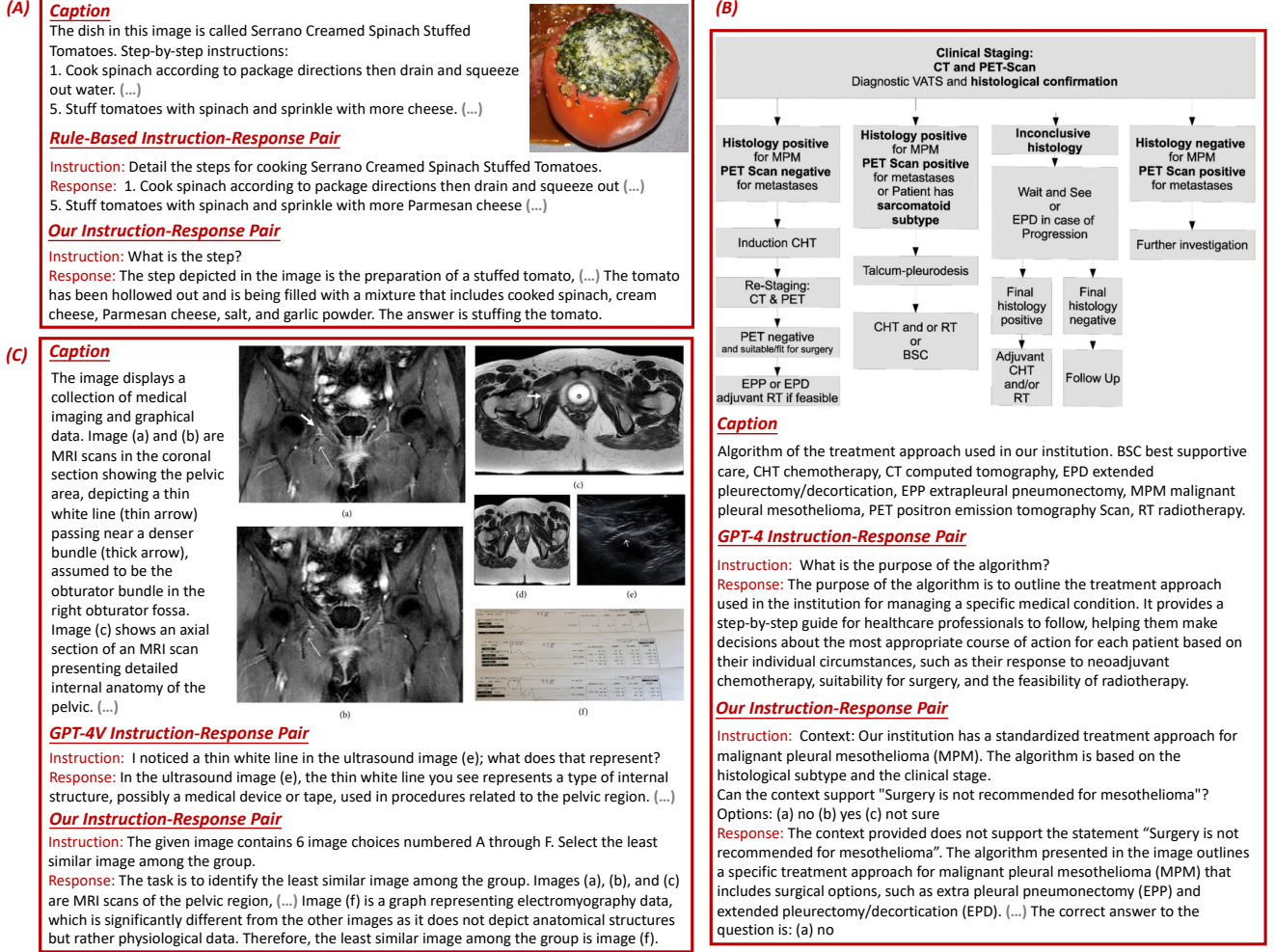


Figure 4. **Cases of Instruction-Response Pairs** synthesized by our method, manual rules, GPT-4, and GPT-4V, the image-caption sources for cases (A), (B), (C) are Recipe1M,  $PMC^{Raw}$  and  $PMC^{Refined}$ , respectively. Certain portions are omitted and are represented as (...).

need for further improvements to enhance response accuracy, even with highly complex tasks.

**Qualitative Analysis** Figure 4 presents cases of synthetic tasks by different methods when given the same image-caption pair. In case (A), the rule-based task is a simple transformation of the recipe caption, ignoring the image information. In contrast, our task conducts a detailed analysis of the food’s state in the image and accurately matches it with the cooking step in the caption, demonstrating a higher level of domain knowledge utilization. In case (B), both our task and the GPT-4 synthesized task focus on interpreting intent. While the GPT-4 task straightforwardly asks for the intent, our task increases task complexity by requiring inference from the context to make a “yes/no/not sure” choice. In case (C) with multiple sub-images, our task type is distinct in requiring the identification of the least similar image among the group, showcasing task diversity. More cases are

provided in Figure 8 in Appendix.

## 8. Conclusion

This paper investigates adapting general MLLMs to specific domains via post-training. To synthesize domain-specific visual instruction tasks, we develop a unified visual instruction synthesizer that generates instruction-response pairs based on domain-specific image-caption data, and then apply a consistency-based filter to improve data accuracy. This enables us to effectively synthesize diverse tasks with high domain knowledge utilization. For the post-training pipeline, we propose combining the synthetic tasks with image-captioning tasks into a single training stage to enhance task diversity. In two domains—biomedicine and food—our resulting model, AdaMLLM, consistently outperforms general MLLMs across various domain-specific tasks. We hope our work can inspire further exploration into MLLM domain adaptation, empowering models for downstream tasks in specialized areas.



## References

- [1] Josh Achiam, Steven Adler, Sandhini Agarwal, Lama Ahmad, Ilge Akkaya, Florencia Leoni Aleman, Diogo Almeida, Janko Altenschmidt, Sam Altman, Shyamal Anadkat, et al. Gpt-4 technical report. *arXiv preprint arXiv:2303.08774*, 2023. 1, 3
- [2] Jean-Baptiste Alayrac, Jeff Donahue, Pauline Luc, Antoine Miech, Iain Barr, Yana Hasson, Karel Lenc, Arthur Mensch, Katherine Millican, Malcolm Reynolds, et al. Flamingo: a visual language model for few-shot learning. *Advances in neural information processing systems*, 35:23716–23736, 2022. 1
- [3] Gagan Bhatia, El Moatez Billah Nagoudi, Hasan Cavusoglu, and Muhammad Abdul-Mageed. Fintral: A family of gpt-4 level multimodal financial large language models. *arXiv preprint arXiv:2402.10986*, 2024. 1
- [4] Lukas Bossard, Matthieu Guillaumin, and Luc Van Gool. Food-101—mining discriminative components with random forests. In *Computer vision—ECCV 2014: 13th European conference, Zurich, Switzerland, September 6–12, 2014, proceedings, part VI 13*, pages 446–461. Springer, 2014. 5, 14
- [5] Tom B Brown. Language models are few-shot learners. *arXiv preprint arXiv:2005.14165*, 2020. 1
- [6] Guiming Hardy Chen, Shunian Chen, Ruifei Zhang, Junying Chen, Xiangbo Wu, Zhiyi Zhang, Zhihong Chen, Jianquan Li, Xiang Wan, and Benyou Wang. Allava: Harnessing gpt4v-synthesized data for a lite vision-language model. *arXiv preprint arXiv:2402.11684*, 2024. 3, 4, 12
- [7] Junying Chen, Ruyi Ouyang, Anningzhe Gao, Shunian Chen, Guiming Hardy Chen, Xidong Wang, Ruifei Zhang, Zhenyang Cai, Ke Ji, Guangjun Yu, et al. Huatuoqpt-vision, towards injecting medical visual knowledge into multimodal llms at scale. *arXiv preprint arXiv:2406.19280*, 2024. 1, 2, 4, 5
- [8] Lin Chen and Long Xing. Open-llava-next: An open-source implementation of llava-next series for facilitating the large multi-modal model community. <https://github.com/xiaoachen98/Open-LLaVA-NeXT>, 2024. 4, 13
- [9] Lin Chen, Jinsong Li, Xiaoyi Dong, Pan Zhang, Conghui He, Jiaqi Wang, Feng Zhao, and Dahua Lin. Sharegpt4v: Improving large multi-modal models with better captions. *arXiv preprint arXiv:2311.12793*, 2023. 13
- [10] Daixuan Cheng, Yuxian Gu, Shaohan Huang, Junyu Bi, Minlie Huang, and Furu Wei. Instruction pre-training: Language models are supervised multitask learners. *arXiv preprint arXiv:2406.14491*, 2024. 1, 2, 7
- [11] Daixuan Cheng, Shaohan Huang, and Furu Wei. Adapting large language models via reading comprehension. In *The Twelfth International Conference on Learning Representations*, 2024. 1
- [12] Aakanksha Chowdhery, Sharan Narang, Jacob Devlin, Maarten Bosma, Gaurav Mishra, Adam Roberts, Paul Barham, Hyung Won Chung, Charles Sutton, Sebastian Gehrmann, et al. Palm: Scaling language modeling with pathways. *Journal of Machine Learning Research*, 24(240): 1–113, 2023. 1
- [13] Thomas G Dietterich. Ensemble methods in machine learning. In *International workshop on multiple classifier systems*, pages 1–15. Springer, 2000. 4
- [14] Abhimanyu Dubey, Abhinav Jauhri, Abhinav Pandey, Abhishek Kadian, Ahmad Al-Dahle, Aiesha Letman, Akhil Mathur, Alan Schelten, Amy Yang, Angela Fan, et al. The llama 3 herd of models. *arXiv preprint arXiv:2407.21783*, 2024. 2, 4, 5
- [15] Xuehai He, Yichen Zhang, Luntian Mou, Eric Xing, and Pengtao Xie. Pathvqa: 30000+ questions for medical visual question answering. *arXiv preprint arXiv:2003.10286*, 2020. 5, 14
- [16] Shaohan Huang, Li Dong, Wenhui Wang, Yaru Hao, Saksham Singhal, Shuming Ma, Tengchao Lv, Lei Cui, Owais Khan Mohammed, Barun Patra, et al. Language is not all you need: Aligning perception with language models. *Advances in Neural Information Processing Systems*, 36:72096–72109, 2023. 1
- [17] Aaron Hurst, Adam Lerer, Adam P Goucher, Adam Perelman, Aditya Ramesh, Aidan Clark, AJ Ostrow, Akila Welihinda, Alan Hayes, Alec Radford, et al. Gpt-4o system card. *arXiv preprint arXiv:2410.21276*, 2024. 5
- [18] Woosuk Kwon, Zhuohan Li, Siyuan Zhuang, Ying Sheng, Lianmin Zheng, Cody Hao Yu, Joseph E. Gonzalez, Hao Zhang, and Ion Stoica. Efficient memory management for large language model serving with pagedattention. In *Proceedings of the ACM SIGOPS 29th Symposium on Operating Systems Principles*, 2023. 12
- [19] Jason J Lau, Soumya Gayen, Asma Ben Abacha, and Dina Demner-Fushman. A dataset of clinically generated visual questions and answers about radiology images. *Scientific data*, 5(1):1–10, 2018. 5, 14
- [20] Yann LeCun. A path towards autonomous machine intelligence. *Open Review*, 2022. 1
- [21] Chen Li, Yixiao Ge, Dian Li, and Ying Shan. Vision-language instruction tuning: A review and analysis. *arXiv preprint arXiv:2311.08172*, 2023. 1, 2
- [22] Chunyuan Li, Cliff Wong, Sheng Zhang, Naoto Usuyama, Haotian Liu, Jianwei Yang, Tristan Naumann, Hoifung Poon, and Jianfeng Gao. Llava-med: Training a large language-and-vision assistant for biomedicine in one day. *Advances in Neural Information Processing Systems*, 36, 2024. 1, 2, 4, 5, 14
- [23] Junnan Li, Dongxu Li, Silvio Savarese, and Steven Hoi. Blip-2: Bootstrapping language-image pre-training with frozen image encoders and large language models. In *International conference on machine learning*, pages 19730–19742. PMLR, 2023. 1
- [24] Ji Lin, Hongxu Yin, Wei Ping, Pavlo Molchanov, Mohammad Sholeybi, and Song Han. Vila: On pre-training for visual language models. In *Proceedings of the IEEE/CVF Conference on Computer Vision and Pattern Recognition*, pages 26689–26699, 2024. 1
- [25] Bo Liu, Li-Ming Zhan, Li Xu, Lin Ma, Yan Yang, and Xiao-Ming Wu. Slake: A semantically-labeled knowledge-enhanced dataset for medical visual question answering. In

- 2021 IEEE 18th International Symposium on Biomedical Imaging (ISBI), pages 1650–1654. IEEE, 2021. 5, 14
- [26] Haotian Liu, Chunyuan Li, Yuheng Li, and Yong Jae Lee. Improved baselines with visual instruction tuning. In *Proceedings of the IEEE/CVF Conference on Computer Vision and Pattern Recognition*, pages 26296–26306, 2024. 4
- [27] Haotian Liu, Chunyuan Li, Yuheng Li, Bo Li, Yuanhan Zhang, Sheng Shen, and Yong Jae Lee. Llava-next: Improved reasoning, ocr, and world knowledge, 2024. 2, 4
- [28] Haotian Liu, Chunyuan Li, Qingyang Wu, and Yong Jae Lee. Visual instruction tuning. *Advances in neural information processing systems*, 36, 2024. 1, 2, 4, 13
- [29] Shayne Longpre, Le Hou, Tu Vu, Albert Webson, Hyung Won Chung, Yi Tay, Denny Zhou, Quoc V Le, Barret Zoph, Jason Wei, et al. The flan collection: Designing data and methods for effective instruction tuning. In *International Conference on Machine Learning*, pages 22631–22648. PMLR, 2023. 4
- [30] Yun Luo, Zhen Yang, Fandong Meng, Yafu Li, Jie Zhou, and Yue Zhang. An empirical study of catastrophic forgetting in large language models during continual fine-tuning. *arXiv preprint arXiv:2308.08747*, 2023. 4, 17
- [31] Yizhen Luo, Jiahuan Zhang, Siqi Fan, Kai Yang, Yushuai Wu, Mu Qiao, and Zaiqing Nie. Biomedgpt: Open multimodal generative pre-trained transformer for biomedicine. *arXiv preprint arXiv:2308.09442*, 2023. 1
- [32] Fnu Mohbat and Mohammed J Zaki. Llava-chef: A multimodal generative model for food recipes. In *Proceedings of the 33rd ACM International Conference on Information and Knowledge Management*, pages 1711–1721, 2024. 1, 2, 4, 5
- [33] Michael Moor, Qian Huang, Shirley Wu, Michihiro Yasunaga, Yash Dalmia, Jure Leskovec, Cyril Zakka, Eduardo Pontes Reis, and Pranav Rajpurkar. Med-flamingo: a multimodal medical few-shot learner. In *Machine Learning for Health (ML4H)*, pages 353–367. PMLR, 2023. 2
- [34] OpenAI. Gpt-4v(ision) system card. 2023. 1, 3
- [35] Zhiliang Peng, Wenhui Wang, Li Dong, Yaru Hao, Shaohan Huang, Shuming Ma, Qixiang Ye, and Furu Wei. Grounding multimodal large language models to the world. In *The Twelfth International Conference on Learning Representations*, 2024. 1
- [36] Alec Radford, Karthik Narasimhan, Tim Salimans, Ilya Sutskever, et al. Improving language understanding by generative pre-training. 2018. 4
- [37] Alec Radford, Jong Wook Kim, Chris Hallacy, Aditya Ramesh, Gabriel Goh, Sandhini Agarwal, Girish Sastry, Amanda Askell, Pamela Mishkin, Jack Clark, et al. Learning transferable visual models from natural language supervision. In *International conference on machine learning*, pages 8748–8763. PMLR, 2021. 1
- [38] Amaia Salvador, Nicholas Hynes, Yusuf Aytar, Javier Marin, Ferda Ofli, Ingmar Weber, and Antonio Torralba. Learning cross-modal embeddings for cooking recipes and food images. In *Proceedings of the IEEE conference on computer vision and pattern recognition*, pages 3020–3028, 2017. 2, 4, 5, 14
- [39] Wenhao Shi, Zhiqiang Hu, Yi Bin, Junhua Liu, Yang Yang, See-Kiong Ng, Lidong Bing, and Roy Ka-Wei Lee. Mathllava: Bootstrapping mathematical reasoning for multimodal large language models. *arXiv preprint arXiv:2406.17294*, 2024. 1
- [40] Guohao Sun, Can Qin, Huazhu Fu, Linwei Wang, and Zhiqiang Tao. Stllava-med: Self-training large language and vision assistant for medical. *arXiv preprint arXiv:2406.19973*, 2024. 1
- [41] Gemini Team, Rohan Anil, Sebastian Borgeaud, Jean-Baptiste Alayrac, Jiahui Yu, Radu Soricut, Johan Schalkwyk, Andrew M Dai, Anja Hauth, Katie Millican, et al. Gemini: a family of highly capable multimodal models. *arXiv preprint arXiv:2312.11805*, 2023. 3
- [42] Quin Thames, Arjun Karpur, Wade Norris, Fangting Xia, Liviu Panait, Tobias Weyand, and Jack Sim. Nutrition5k: Towards automatic nutritional understanding of generic food. In *Proceedings of the IEEE/CVF Conference on Computer Vision and Pattern Recognition*, pages 8903–8911, 2021. 5, 14
- [43] Shengbang Tong, Ellis Brown, Penghao Wu, Sanghyun Woo, Manoj Middepogu, Sai Charitha Akula, Jihan Yang, Shusheng Yang, Adithya Iyer, Xichen Pan, et al. Cambrian-1: A fully open, vision-centric exploration of multimodal llms. *arXiv preprint arXiv:2406.16860*, 2024. 1
- [44] Hugo Touvron, Thibaut Lavril, Gautier Izacard, Xavier Martinet, Marie-Anne Lachaux, Timothée Lacroix, Baptiste Rozière, Naman Goyal, Eric Hambro, Faisal Azhar, et al. Llama: Open and efficient foundation language models. *arXiv preprint arXiv:2302.13971*, 2023. 1
- [45] Peng Wang, Shuai Bai, Sinan Tan, Shijie Wang, Zhihao Fan, Jinze Bai, Keqin Chen, Xuejing Liu, Jialin Wang, Wenbin Ge, et al. Qwen2-vl: Enhancing vision-language model’s perception of the world at any resolution. *arXiv preprint arXiv:2409.12191*, 2024. 2, 5
- [46] Xuezhi Wang, Jason Wei, Dale Schuurmans, Quoc Le, Ed Chi, Sharan Narang, Aakanksha Chowdhery, and Denny Zhou. Self-consistency improves chain of thought reasoning in language models. *arXiv preprint arXiv:2203.11171*, 2022. 4
- [47] Jason Wei, Maarten Bosma, Vincent Y Zhao, Kelvin Guu, Adams Wei Yu, Brian Lester, Nan Du, Andrew M Dai, and Quoc V Le. Finetuned language models are zero-shot learners. *arXiv preprint arXiv:2109.01652*, 2021. 4
- [48] Jason Wei, Xuezhi Wang, Dale Schuurmans, Maarten Bosma, Fei Xia, Ed Chi, Quoc V Le, Denny Zhou, et al. Chain-of-thought prompting elicits reasoning in large language models. *Advances in neural information processing systems*, 35:24824–24837, 2022. 3
- [49] Xiongwei Wu, Xin Fu, Ying Liu, Ee-Peng Lim, Steven CH Hoi, and Qianru Sun. A large-scale benchmark for food image segmentation. In *Proceedings of the 29th ACM international conference on multimedia*, pages 506–515, 2021. 5, 14
- [50] Qianqian Xie, Dong Li, Mengxi Xiao, Zihao Jiang, Ruoyu Xiang, Xiao Zhang, Zhengyu Chen, Yueru He, Weiguang Han, Yuzhe Yang, et al. Open-finllms: Open multimodal

- large language models for financial applications. *arXiv preprint arXiv:2408.11878*, 2024. [1](#)
- [51] Zhiyang Xu, Chao Feng, Rulin Shao, Trevor Ashby, Ying Shen, Di Jin, Yu Cheng, Qifan Wang, and Lifu Huang. Vision-flan: Scaling human-labeled tasks in visual instruction tuning. *arXiv preprint arXiv:2402.11690*, 2024. [3](#), [4](#), [12](#)
- [52] Yuan Yao, Tianyu Yu, Ao Zhang, Chongyi Wang, Junbo Cui, Hongji Zhu, Tianchi Cai, Haoyu Li, Weilin Zhao, Zhihui He, et al. Minicpm-v: A gpt-4v level mllm on your phone. *arXiv preprint arXiv:2408.01800*, 2024. [1](#)
- [53] Yuehao Yin, Huiyan Qi, Bin Zhu, Jingjing Chen, Yu-Gang Jiang, and Chong-Wah Ngo. Foodlmm: A versatile food assistant using large multi-modal model. *arXiv preprint arXiv:2312.14991*, 2023. [2](#)
- [54] Pan Zhang, Xiaoyi Dong, Bin Wang, Yuhang Cao, Chao Xu, Linke Ouyang, Zhiyuan Zhao, Haodong Duan, Songyang Zhang, Shuangrui Ding, et al. Internlm-xcomposer: A vision-language large model for advanced text-image comprehension and composition. *arXiv preprint arXiv:2309.15112*, 2023. [1](#)
- [55] Sheng Zhang, Yanbo Xu, Naoto Usuyama, Jaspreet Bagga, Robert Tinn, Sam Preston, Rajesh Rao, Mu Wei, Naveen Valluri, Cliff Wong, et al. Large-scale domain-specific pre-training for biomedical vision-language processing. *arXiv preprint arXiv:2303.00915*, 2(3):6, 2023. [4](#)
- [56] Wei Zhang, Miaoxin Cai, Tong Zhang, Yin Zhuang, and Xuerui Mao. Earthgpt: A universal multi-modal large language model for multi-sensor image comprehension in remote sensing domain. *IEEE Transactions on Geoscience and Remote Sensing*, 2024. [1](#)
- [57] Xiaoman Zhang, Chaoyi Wu, Ziheng Zhao, Weixiong Lin, Ya Zhang, Yanfeng Wang, and Weidi Xie. Pmc-vqa: Visual instruction tuning for medical visual question answering. *arXiv preprint arXiv:2305.10415*, 2023. [2](#), [5](#), [14](#)
- [58] Zhenliang Zhang, Zeyu Zhang, Ziyuan Jiao, Yao Su, Hangxin Liu, Wei Wang, and Song-Chun Zhu. On the emergence of symmetrical reality. In *Proceedings of the IEEE Conference Virtual Reality and 3D User Interfaces (VR)*, pages 639–649. IEEE, 2024. [1](#)
- [59] Henry Hengyuan Zhao, Pan Zhou, and Mike Zheng Shou. Genixer: Empowering multimodal large language models as a powerful data generator. *arXiv preprint arXiv:2312.06731*, 2023. [2](#), [7](#)
- [60] Yaowei Zheng, Richong Zhang, Junhao Zhang, Yanhan Ye, Zheyang Luo, Zhangchi Feng, and Yongqiang Ma. Llamafactory: Unified efficient fine-tuning of 100+ language models. In *Proceedings of the 62nd Annual Meeting of the Association for Computational Linguistics (Volume 3: System Demonstrations)*, Bangkok, Thailand, 2024. Association for Computational Linguistics. [13](#)

## Appendix

### A. Seed Data Construction and Distribution

We convert the combination of VisionFLAN [51] and ALLaVA [6] into our required format. Each seed data example consists of an image-caption pair as the input and a related task triplet as the output, which includes an instruction, an informative response, and a precise response. VisionFLAN is a human-annotated visual instruction task dataset containing 191 tasks, each with 1K examples. ALLaVA builds on VisionFLAN by using GPT-4V to generate a caption for each image and to regenerate a response for each instruction. In our format, the image, instruction, and human-annotated response from VisionFLAN are used as the image, instruction, and precise response, respectively, while the caption and GPT-4V regenerated response from ALLaVA are used as the caption and informative response. Benefiting from the diversity of existing datasets, our seed data encompass a wide range of image domains and task types, as shown in Figure 5.

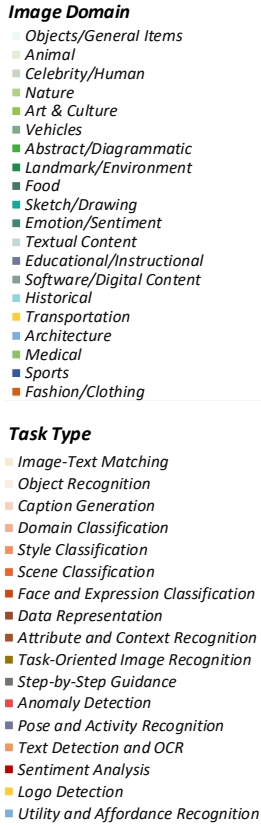


Figure 5. **Distribution of Image Domains and Task Types in Seed Data.**

### B. Implementation Details of Visual Instruction Synthesis

Table 9 presents the hyper-parameters used for synthesizer tuning. We employ the vLLM inference framework [18] to speed up task synthesis and consistency checks. On a single A100-80GB GPU, it takes approximately 10 hours to synthesize task triplets and an additional 2.5 hours to perform consistency-based filtering for every 100K image-caption pairs. After applying consistency-based filtering, we collect 150K, 144K, and 32K instruction-response pairs for  $PMC^{Raw}$ ,  $PMC^{Refined}$ , and Recipe1M, respectively.

Hyper-Parameter	Assignment
Base Model	LLaVA-v1.6-8B
Trainable	Full Model
Epoch	2
Batch Size	128
Max Seq Length	6144
LR <sub>projector &amp; LLM</sub>	2e-5
LR <sub>visual encoder</sub>	2e-6
LR Scheduler	Cosine
Weight Decay	0
Warm-Up Ratio	0.03
Computing Infrastructure	8 A100-80GB GPUs
Training Time	13 Hours

Table 9. **Hyper-Parameters for Synthesizer Tuning**

MLLM	LLaVA-v1.6	Qwen2-VL	Llama-3.2
Trainable	Full Model	Full Model	Full Model
Epoch	1	1	1
Batch Size	128	128	128
Max Seq Length	6144	6144	6144
LR <sub>projector &amp; LLM</sub>	2e-5	1e-5	5e-6
LR <sub>visual encoder</sub>	2e-6	1e-5	5e-6
LR Scheduler	Cosine	Cosine	Cosine
Weight Decay	0	0.1	0.1
Warm-Up Ratio	0.03	0.1	0.1

Table 10. **Hyper-Parameters for MLLM Single-Stage Post-Training.**

Image-Caption	$PMC^{Raw}$	$PMC^{Refined}$	Recipe1M
LLaVA-v1.6-8B	21	23	6
Qwen2-VL-2B	3.5	4	1
Llama-3.2-11B	29	31	9

Table 11. **Training Time (Hours) for MLLM Single-Stage Post-Training** on 8 A100-80GB GPUs.



## C. MLLM Post-Training Settings and Costs

Tables 10 and 11 present the hyper-parameters and training time for the single-stage post-training of MLLMs. In the two-stage training experiments, we employ two common approaches for the first stage on image-caption pairs: (1) unfreezing only the vision-language projector [28] for LLaVA-v1.6-8B, and (2) unfreezing the full model [9] for Qwen2-VL-2B and Llama-3.2-11B. During the second stage on visual instruction tasks, we unfreeze the full model across all setups. The hyperparameters for both stages on Qwen2-VL-2B and Llama-3.2-11B are the same as those listed in the table. For LLaVA-v1.6-8B, the first stage differs only in the trainable module, which is the vision-language projector, using a learning rate of  $2e-3$ . The hyperparameters for the second stage are the same as those listed in the table. We use the code implementations from [8] for experiments on LLaVA-v1.6-8B and from [60] for experiments on Qwen2-VL-2B and Llama-3.2-11B.

## D. Scoring Criteria for Data Quality

For each synthetic dataset, we sample 200 examples and use the following scoring criteria to evaluate data quality in each aspect. The final scores are rescaled to a 0-100 range for presentation uniformity.

**Task Diversity** For each instruction-response pair, the annotator selects the most appropriate category from the common vision instruction task types listed below. Once all data samples are annotated, we report the number of distinct task types normalized by the total number of common task types.

- *Domain Classification*: Classifying images into domains like race, animal categories, and environment types.
- *Object Recognition*: Recognizing detailed objects like animal species, car brands, and specific object types.
- *Pose and Activity Recognition*: Identifying specific human poses and activities.
- *Logo Detection*: Detecting and recognizing brand logos.
- *Face and Expression Classification*: Classifying facial attributes by age, gender, and detecting expressions.
- *Scene Classification*: Categorizing images into scene types like beaches, forests, and cities.
- *Sentiment Analysis*: Detecting sentiment in images.
- *Caption Generation*: Generating captions for images, including general and contextual descriptions.
- *Text Detection and OCR*: Recognizing text in images and structured text detection.
- *Image-Text Matching*: Assessing image-text similarity and coherence for multimodal content.
- *Anomaly Detection*: Identifying anomalies in settings like industrial and road scenes.
- *Style Classification*: Classifying images by artistic style and quality.

- *Attribute and Context Recognition*: Detecting image attributes and contexts, such as object presence and temporal classification.
- *Task-Oriented Image Recognition*: Recognizing objects in structured contexts, like weed species and quick-draw sketches.
- *Step-by-Step Guidance*: Recognizing steps in instructional content, like wikiprocedures.
- *Data Representation and Visualization*: Visual QA for charts and chart captioning.
- *Utility and Affordance Recognition*: Detecting object utility or affordance in images.
- *Visual Grounding*: Linking image parts to corresponding words or phrases.
- *Segmentation*: Dividing images into meaningful segments, identifying objects or regions.
- *Visual Storytelling*: Creating narratives based on a series of images.

**Domain Knowledge Utilization** For each instruction-response pair, the annotator evaluates the extent to which domain-specific knowledge from the image is utilized to complete the task. The scoring follows the criteria below, and we report the average score across all samples.

- 1: The task is totally irrelevant to the image.
- 2: The task is relevant, but the question is mundane and answerable without reviewing the image.
- 3: The task requires reviewing the image, but the question is vague, such as asking for a general caption.
- 4: The task is clear, but the question focuses on only one detail in the image.
- 5: The task is highly relevant to both the details and overall context of the image.

**Task Complexity** For each instruction-response pair, the annotator assesses task complexity, with higher scores for tasks requiring reasoning and instruction-following abilities, using the criteria below. We report the average score across all samples.

- 1: The task can be easily completed by mimicking part of the caption.
- 2: The task can be easily completed by reviewing the image, such as identifying an obvious object.
- 3: The task requires consideration of the details.
- 4: The task requires complex reasoning on details and overview.
- 5: The task requires complex reasoning and instruction-following abilities, such as returning the answer in a required format.

**Response Accuracy** For each instruction-response pair, the annotator assesses whether the response correctly ad-

addresses the task based on the context, using the following criteria. We report the average score across all samples.

- 1: The response is totally irrelevant to the task instruction.
- 2: The response attempts to address the instruction, but both the reasoning and conclusion are incorrect.
- 3: The reasoning is correct, but the conclusion is incorrect.
- 4: The conclusion is correct, but the reasoning is incorrect.
- 5: Both the reasoning and conclusion are correct.

## E. Task Evaluation Details

Tables 12 and 13 present the specifications and prompt templates for evaluated tasks in each domain. We conduct zero-shot prompting evaluations on these tasks.

For biomedicine, we follow the evaluation approach of [22] for SLAKE, PathVQA, and VQA-RAD, and the method of [57] for PMC-VQA.

- *SLAKE* [25] is a semantically-labeled, knowledge-enhanced medical VQA dataset with radiology images and diverse QA pairs annotated by physicians. The dataset includes semantic segmentation masks, object detection bounding boxes, and covers various body parts. “CLOSED” answers are yes/no type, while “OPEN” answers are one-word or short phrases. We use only the English subset.
- *PathVQA* [15] consists of pathology images with QA pairs covering aspects like location, shape, and color. Questions are categorized as “OPEN” (open-ended) or “CLOSED” (closed-ended).
- *VQA-RAD* [19] includes clinician-generated QA pairs and radiology images spanning the head, chest, and abdomen. Questions are categorized into 11 types, with answers as either “OPEN” (short text) or “CLOSED” (yes/no).
- *PMC-VQA* [57] is larger and more diverse MedVQA

datasets, with questions ranging from identifying modalities and organs to complex questions requiring specialized knowledge. All questions are multiple-choice.

For the food domain, the task descriptions are as follows:

- *Recipe1M* [38] contains recipe information, including titles, ingredients, and cooking instructions. We evaluate models by taking an image and asking for the recipe name, ingredients, and steps.
- *Nutrition5K* [42] comprises real-world food dishes with RGB images and nutritional content annotations. We use the ingredient information to create an ingredient prediction task, where the model generates ingredients from an image.
- *Food101* [4] features images across 101 food categories. We ask the model to classify each image into one of the 101 categories.
- *FoodSeg103* [49] includes 103 food categories with images and pixel-wise ingredient annotations. We ask the model to select one or multiple categories from a provided list.

Task	Description	Metric	Test Num
<i>BioMed.</i>			
SLAKE OPEN [25]	Medical question answering	Recall	645
SLAKE CLOSED [25]	Medical binary classification	Accuracy	416
PathVQA OPEN [15]	Medical question answering	Recall	3357
PathVQA CLOSED [15]	Medical binary classification	Accuracy	3362
VQA-RAD OPEN [19]	Medical question answering	Recall	179
VQA-RAD CLOSED [19]	Medical binary classification	Accuracy	272
PMC-VQA [57]	Medical multi-choice QA	Accuracy	2000
<i>Food</i>			
Recipe1M [38]	Recipe generation	Rouge-L	1000
Nutrition5K [42]	Ingredient prediction	Recall	507
Food101 [4]	Food category classification	Accuracy	25250
FoodSeg103 [49]	Food multi-label classification	F1	2135

Table 12. Specifications of the Evaluated Domain-Specific Task Datasets.

Task	Instruction	Response
<i>BioMed.</i>		
SLAKE	{question}	{answer}
PathVQA	{question}	{answer}
VQA-RAD	{question}	{answer}
PMC-VQA	Question: {question} The choices are: {options}	{option}
<i>Food</i>		
Recipe1M	{question}	{recipe}
Nutrition5K	What ingredients are used to make the dish in the image?	{ingredients}
Food101	What type of food is shown in this image? Choose one type from the following options: {food type options}	{food type}
FoodSeg103	Identify the food categories present in the image. The available categories are: {options} Please return a list of the selected food categories, formatted as a list of names like [candy, egg tart, french fries, chocolate].	{categories}

Table 13. Prompt Templates of the Evaluated Domain-Specific Task Datasets.

I have an image-related question for which I have received two answers: one is informative, and the other is precise. Please help me assess whether the precise answer is consistent with the informative answer.

Below are some examples. For each example, write your judgement as follows:

- Yes: Consistent, meaning the precise answer can be inferred from the informative answer.
- No: Inconsistent, meaning the precise answer cannot be inferred from the informative answer.
- Open: Indicates that the question invites multiple interpretations or that answers can be expressed through open-ended phrasing, acknowledging complexity, or encouraging personal perspectives. It is also applicable to questions that require image description, captions, or background knowledge.

## Question: Given an image of something from the kitchen, identify what it could be. The image could be of cooking tools or items that are used for eating. It could also be used for serving food or storing it.  
Options: (a) This image contains a cup (b) This image contains a bottle (c) This image contains a knife (d) This image contains a wine glass (e) This image contains a spoon (f) This image contains a bowl (g) This image contains a fork

## Informative Answer: The options provided relate to identifying kitchenware or items related to food service. From the given list, the most clearly identifiable object in the image is a plastic bottle with a blue label, which is visible in the background behind the dishes. No cups, knives, wine glasses, spoons, bowls (in the sense of a single, empty bowl), or forks are distinctly visible. Therefore, the correct identification from the provided options is:  
(b) This image contains a bottle.

## Precise Answer: (a) This image contains a cup

## Consistent: No

## Question: You are provided with an image which contains two pictures side by side. Your task is to identify the differences between the two pictures. Separate the differences with a comma.

## Informative Answer: Upon close inspection, the differences between the two images are subtle but distinct. The shadows cast by the trees and lamp posts differ in length and direction, suggesting a slight variation in the time or position of the sun when the photos were taken. The arrangement and presence of cars vary\u2014some are present in one image but not in the other. Architectural details such as windows, roof lines, and the design on the building exteriors also show discrepancies. The color of the roof on the small central structure is different in each picture, with one appearing darker than the other. Lastly, the patterns on the sidewalks, especially the crosswalk lines, are not identical, indicating a variation in either the perspective or actual changes in the environment.

## Precise Answer: the redish brown car moves slightly.

## Consistent: Open

Figure 6. Prompt Template for Consistency-Based Filter (Part 1), continued in Part 2.

```

## Question: Given an image of an animal, identify the kind of animal in the image. The picture could
be of more popular animals that are visible around zoos or are sometimes domesticated at home. They
could also sometimes be found in the wild.\nOptions: (a) This image contains a zebra (b) This image
contains a cow (c) This image contains a horse (d) This image contains an elephant (e) This image
contains a giraffe (f) This image contains a sheep (g) This image contains a cat (h) This image
contains a bear (i) This image contains a bird (j) This image contains a dog
## Informative Answer: The animal in the image can be identified as a dog, specifically a golden
retriever. This determination is based on several visual cues such as the golden coat, the size and
shape of the ears, the facial structure, and the overall body size, which are characteristic of this
breed. Golden retrievers are a popular domesticated breed known for their friendly and intelligent
demeanor. They are commonly kept as pets and are not typically found in zoos or in the wild. The image
does not contain any of the other animals listed in the options (a) through (i).
## Precise Answer: (j) This image contains a dog
## Consistent: Yes

## Question: Question: Is the picture taken outdoors?\nPlease answer the question by analyzing the
scene in the provided image.
## Informative Answer: Analyzing the elements within the image, there are several indicators confirming
that the picture is taken outdoors. The presence of natural elements like grass, trees, and the open
sky, along with architectural features that are not enclosed, such as the adobe-style building with
exterior walls and windows, support this observation. The lighting and shadows cast by the trees are
consistent with natural sunlight, further corroborating the outdoor setting. Moreover, the materials
used in the path and bench are typical of outdoor furnishings, designed to withstand weather conditions.
All these aspects contribute to the conclusion that the photograph was taken in an exterior space,
likely a garden or park associated with the building in the background.
## Precise Answer: yes
## Consistent: Yes

## Question: This task tests your ability to count number of objects. Here is the question \"How many
chairs are in the photo?\"
## Informative Answer: Upon careful observation of the photo, each individual is seated in a distinct
chair. The positioning of the subjects and their engagement with the camera suggests they are occupying
all the chairs present at their table. There are no other chairs discernible in the immediate vicinity
of the table or in the background. Therefore, it can be concluded that there are exactly four chairs in
the photo, corresponding to the four people seen around the table.
## Precise Answer: two
## Consistent: No

## Question: Can you give me a caption and some background knowledge about this image?
## Informative Answer: A detailed caption for this image could read: \"A moment of reflection and
accomplishment, as a retired NBA All-Star sits with the Championship Trophy, surrounded by peers and
the spirit of the game.\" The image is probably taken at an NBA event dedicated to honoring the
achievements of past basketball legends. The trophy next to the man symbolizes the pinnacle of success
in the league, suggesting that he may be one of the accomplished players who has reached this level of
success. The attire of the individuals indicates a formal celebration of basketball history, and the
relaxed atmosphere hints at a session of storytelling or interviews about their experiences in the
sport.\"
## Precise Answer: Moses Malone was selected by the New Orleans Jazz with the first pick. On December 9,
1975, the NBA planned to host a supplementary draft to settle negotiating rights to five ABA players
who had never been eligible for the NBA draft because their college classes had not graduated and they
had not apply for hardship. The teams selected in reverse order of their winloss record in the previous
season. The team that made a selection must withdraw their equivalent selection in the 1976 Draft. The
teams were allowed to not exercise their rights on this hardship draft and thus retained their full
selection in the 1976 Draft. The draft itself attracted strong opposition from the ABA who accuse the
NBA trying to reduce confidence in the stability of their league. Despite the initial postponement of
the draft, the draft was finally held on December 30, 1975.
## Consistent: Open

## Question: {Instruction}
## Informative Answer: {Informative Response}
## Precise Answer: {Precise Response}
## Consistent:

```

Figure 7. Prompt Template for Consistency-Based Filter (Part 2).



<b>Recipe1M</b>	<i>Train Pipeline</i>	Instruction	<b>Recipe</b>	<b>Nutrition</b>	<b>Food101</b>	<b>FoodSeg</b>	<b>AVERAGE</b>
LLaVA-v1.6-8B	<i>Two-Stage</i>	Rule	23.1	29.1	46.8	14.5	28.4
		Ours	16.2	28.3	43.5	28.0	29.0
	<i>Single-Stage</i>	Rule	21.8	36.7	63.9	13.9	34.1
		Ours	24.8	36.1	65.3	42.0	42.0
Qwen2-VL-2B	<i>Two-Stage</i>	Rule	24.1	24.5	68.8	7.7	31.3
		Ours	16.5	43.0	69.5	23.9	38.2
	<i>Single-Stage</i>	Rule	19.3	37.1	64.7	6.6	31.9
		Ours	24.0	41.2	72.0	23.9	40.3
Llama-3.2-11B	<i>Two-Stage</i>	Rule	25.7	26.2	82.1	16.7	37.7
		Ours	17.8	38.0	74.6	33.2	40.9
	<i>Single-Stage</i>	Rule	21.4	32.2	75.8	16.9	36.6
		Ours	26.1	41.0	82.2	42.0	47.8

<b>PMC<sup>Raw</sup></b>	<i>Train Pipeline</i>	Instruction	<b>SLAKE</b>		<b>PathVQA</b>		<b>VQA-RAD</b>		<b>PMC-VQA</b>	<b>AVERAGE</b>
			OPEN	CLOSED	OPEN	CLOSED	OPEN	CLOSED		
LLaVA-v1.6-8B	<i>Two-Stage</i>	GPT-4	43.4	50.2	10.1	59.2	35.0	62.5	37.1	42.5
		Ours	56.2	71.4	17.2	74.5	50.6	79.0	40.4	55.6
	<i>Single-Stage</i>	GPT-4	44.2	59.1	11.6	62.2	38.5	67.3	39.9	46.1
		Ours	56.8	76.4	19.7	79.3	51.0	80.5	44.3	58.3
Qwen2-VL-2B	<i>Two-Stage</i>	GPT-4	43.4	55.5	11.8	60.1	37.1	58.8	41.2	44.0
		Ours	55.2	74.5	18.4	68.4	48.8	79.8	43.8	55.5
	<i>Single-Stage</i>	GPT-4	43.6	59.6	13.2	47.4	37.3	57.0	31.2	41.3
		Ours	53.2	75.2	20.1	63.8	49.8	74.6	43.5	54.3
Llama-3.2-11B	<i>Two-Stage</i>	GPT-4	47.6	58.7	14.6	69.5	38.0	69.1	47.5	49.3
		Ours	60.0	75.7	22.1	76.8	51.4	80.5	47.9	59.2
	<i>Single-Stage</i>	GPT-4	46.8	56.5	16.0	69.9	41.9	65.4	45.3	48.8
		Ours	56.7	77.6	22.2	87.3	55.0	76.1	49.9	60.7

<b>PMC<sup>Refined</sup></b>	<i>Train Pipeline</i>	Instruction	<b>SLAKE</b>		<b>PathVQA</b>		<b>VQA-RAD</b>		<b>PMC-VQA</b>	<b>AVERAGE</b>
			OPEN	CLOSED	OPEN	CLOSED	OPEN	CLOSED		
LLaVA-v1.6-8B	<i>Two-Stage</i>	GPT-4V	50.0	68.3	17.0	67.5	43.3	67.3	40.4	50.5
		Ours	54.8	73.1	19.3	79.7	55.6	82.7	45.1	58.6
	<i>Single-Stage</i>	GPT-4V	52.3	76.2	20.1	73.3	47.0	76.5	43.1	55.5
		Ours	58.0	73.3	22.9	78.6	59.8	81.3	47.9	60.3
Qwen2-VL-2B	<i>Two-Stage</i>	GPT-4V	45.2	63.2	18.2	64.7	41.3	67.3	43.2	49.0
		Ours	60.8	76.9	21.4	75.0	55.0	82.7	44.7	59.5
	<i>Single-Stage</i>	GPT-4V	51.4	66.1	18.9	61.4	45.1	73.2	45.1	51.6
		Ours	60.2	75.0	20.6	53.6	58.0	76.1	46.5	55.7
Llama-3.2-11B	<i>Two-Stage</i>	GPT-4V	49.1	74.3	19.3	70.9	46.2	73.9	47.1	54.4
		Ours	58.5	76.4	27.0	73.2	58.3	77.6	51.3	60.3
	<i>Single-Stage</i>	GPT-4V	47.1	72.6	19.5	70.7	45.9	73.9	46.5	53.7
		Ours	59.5	76.4	24.3	84.9	57.4	79.8	51.9	62.0

Table 14. **Domain-Specific Task Performance of MLLMs after Post-Training** with different synthetic data and training pipelines. The image-caption sources are Recipe1M, PMC<sup>Raw</sup> and PMC<sup>Refined</sup>, respectively. In most cases using our synthetic data, we find that single-stage training outperforms two-stage training on domain-specific tasks, particularly evident in the **Recipe** generation results for the food domain. Recall that in the two-stage training approach for the food domain, the model first trains on recipe captions and then on our synthetic tasks. We examine the task performance of LLaVA-v1.6-8B on **Recipe** generation and observe that the model achieves a score of 25.3 after the first stage on recipe captions. However, this score drastically decreases to 16.2 after the second stage. From this, we infer that the two-stage approach causes the model to catastrophically forget the task/knowledge learned in the first stage when transitioning to the second stage [30], leading to poorer performance after completing the second-stage training.

### Caption

To make Evie'S Ranch Nuggets, you'll need these ingredients: (1). 2 pounds skinless, boneless chicken breasts, cut into 2 inch pieces (2). 1/2 cup sour cream (3). 1/2 cup all-purpose flour (4). 4 ounces Ranch-flavored tortilla chips (5). vegetable cooking spray

Follow these steps to cook it:

[+] Preheat the oven to 400 degrees F (200 degrees C). Line a baking sheet with aluminum foil.

[+] Place tortilla chips and flour into a food processor or blender, and process into crumbs. Pour into a bowl. Place chicken pieces into a sealable plastic bag with sour cream. Massage the bag to make sure chicken pieces are coated with sour cream. Let sit for 5 minutes.

[+] Dip coated chicken pieces into the chip crumbs, and place on the prepared baking sheet. Spray lightly with vegetable cooking spray.

[+] Bake for 30 minutes in the preheated oven, until chicken is cooked through and juices run clear.



### Rule-Based Instruction-Response Pair

**Instruction:** I'm curious! What's the name, ingredients, and cooking method for this mouth-watering creation?

**Response:** To make Evie'S Ranch Nuggets, you'll need these ingredients: (1). 2 pounds skinless, boneless chicken breasts, cut into 2 inch pieces (2). 1/2 cup sour cream (3). 1/2 cup all-purpose flour (4). 4 ounces Ranch-flavored tortilla chips (5). vegetable cooking spray  
Follow these steps to cook it:

[+] Preheat the oven to 400 degrees F (200 degrees C). Line a baking sheet with aluminum foil. (...)

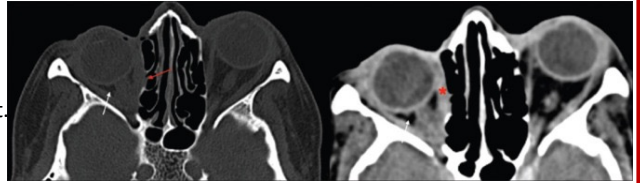
### Our Instruction-Response Pair

**Instruction:** Texture is defined as the feel, appearance or consistency of a surface or substance from a human's perspective. Detect the primary texture represented in the image.

**Response:** The primary texture represented in the image is that of a crispy, crunchy exterior typical of fried foods. The uneven, rough surface of the chicken nuggets suggests a firm texture that would be audible upon bite. The golden-brown color indicates a Maillard reaction, which is a chemical reaction between amino acids and reducing sugars that gives browned food its distinctive flavor. This reaction also contributes to the crunchy texture, as it creates a rigid outer layer. The visible crumbs and the rough, uneven surface further emphasize the crunchy texture that one would expect from such a food item.

### Caption

CT scan of the orbits revealed right eye enophthalmos, focal osseous defect of lamina papyracea (red arrow), deficient orbital fat (white arrow), fibrosis of soft tissue (red star) along medial wall of right orbit.



### GPT-4 Instruction-Response Pair

**Instruction:** What is the red arrow pointing to?

**Response:** The red arrow in the CT scan is pointing to a focal osseous defect of the lamina papyracea.

### Our Instruction-Response Pair

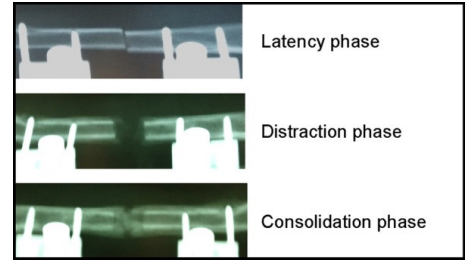
**Instruction:** What is the location of the lesion?

**Response:** The lesion is located in the right orbit. On the CT scan, it appears as an area of increased density (hyperdense) relative to the surrounding brain tissue. The lesion is situated medial to the eyeball, which is the most prominent structure within the orbit. It is important to note that the interpretation of radiological images should be performed by a qualified radiologist, as it requires a detailed understanding of human anatomy and the ability to correlate findings with clinical symptoms for an accurate diagnosis. The answer is right orbit.

Figure 8. **Cases of Instruction-Response Pairs (Part 1)** synthesized by our method, manual rules, GPT-4, and GPT-4V, the image-caption sources for the cases are Recipe1M, PMC<sup>Raw</sup> and PMC<sup>Refined</sup>, respectively. Continued in Part 2. In the first case, the rule-based task simply transforms the recipe caption, ignoring the image content. In contrast, our task involves analyzing the food's state in the image and applying food-related knowledge to infer its texture, demonstrating a higher level of domain knowledge utilization. In the second case, the GPT-4 generated task straightforwardly asks about the pointing of the red arrow, while ours requires a detailed analysis and inference, showing greater task complexity.

### Caption

The image displays three distinct panels, each labeled with a different phase of bone development under distraction osteogenesis. The top panel, labeled 'Latency phase', shows an X-ray image of a bone with a surgical device composed of two parallel metal plates attached by screws on either side of a bone segment. The middle panel, labeled 'Distraction phase', depicts the same bone but with a noticeable increase in the gap between the bone ends, suggesting bone lengthening. The bottom panel, labeled 'Consolidation phase', illustrates further progress of bone growth within the gap, indicating new bone formation and consolidation. Each panel uses the same angle and lighting conditions to emphasize the changes in the bone structure across different phases.



### GPT-4V Instruction-Response Pair

**Instruction:** Can you identify the type of surgical hardware used in these phases based on the image, and explain its role in the manipulation of bone segments during distraction osteogenesis?

**Response:** The surgical hardware visualized in the image appears to be a type of external fixator, consisting of two parallel metal plates connected by screws that penetrate through the bone segments. This hardware plays a pivotal role in distraction osteogenesis by stabilizing the bone while also allowing for gradual bone lengthening. The screws can be adjusted to manipulate the distance between the divided bone segments, facilitating new bone growth in the process required by the distraction phase.

### Our Instruction-Response Pair

**Instruction:** What is the gap between the bone ends called?

The choices are: (A) Consolidation; (B) Distraction; (C) Latency; (D) None of the above.

**Response:** The gap between the bone ends, as depicted in the middle panel of the image, is referred to as the 'Distraction phase'. This phase is characterized by the lengthening of the bone due to the application of a distraction device, which separates the bone ends and allows for new bone growth to fill the gap. Therefore, the correct answer to the question is: (B) Distraction.

Figure 9. **Cases of Instruction-Response Pairs (Part 2)** synthesized by our method, manual rules, GPT-4, and GPT-4V, the image-caption sources for the cases are Recipe1M,  $PMC^{Raw}$  and  $PMC^{Refined}$ , respectively. In this case, our task stands out as a multiple-choice question, showcasing task diversity.